Indonesian Journal of Electrical Engineering and Computer Science
Vol. 40, No. 3, December 2025, pp. 1212~1220
ISSN: 2502-4752, DOI: 10.11591/ijeecs.v40.i3.pp1212-1220

FEM-based analysis of the relationship between track insulation conductivity and stray current in DC traction systems

Apiwat Aussawamaykin, Padej Pao-la-or
School of Electrical Engineering, Institute of Engineering, Suranaree University of Technology, Nakhon Ratchasima, Thailand

Article Info

Article history:

Received Oct 3, 2024
Revised Oct 16, 2025
Accepted Nov 16, 2025

Keywords:

DC traction system
Finite element method
Rail fastening
Stray current
Track insulation measurement

ABSTRACT

This research investigates the influence of track insulation conductivity on stray current in direct current (DC) traction systems, which is a significant issue in railway operations due to its potential to cause electrochemical corrosion. Utilizing the finite element method (FEM), a simplified geometric model of a DC tram traction system was analyzed under varying conditions of track insulation conductivity. The study examined three levels of insulation conductivity, represented by fastener resistances of 1,000 Ω, 3,000 Ω, and 6,000 Ω, to understand their impact on stray current density. Results revealed that increased insulation resistance leads to reduced stray current density, demonstrating the critical role of track insulation in mitigating stray currents. The study further highlights that the depth of soil beneath the track also significantly affects stray current distribution. These findings provide insights into improving track design and maintenance for better protection against the negative effects of stray current in DC traction systems.

Corresponding Author:

Padej Pao-la-or
School of Electrical Engineering, Institute of Engineering, Suranaree University of Technology
Nakhon Ratchasima, Thailand
Email: padej@sut.ac.th

1. INTRODUCTION

In light railways, metros, and rapid transit (MRT) systems, which use direct current (DC) traction, power is supplied to trains through an overhead catenary system (OCS), third rail, or power rail. The return path for the current is provided by the running rails, which direct it back to the supply source [1]. However, as rail-to-ground insulation degrades, some current leaks into the ground and flows back to the DC traction substation as shown in Figure 1 [2]. This leakage current, known as stray current [3], causes electrochemical corrosion, which affects buried metals such as gas pipelines [4]. This occurs when cations and electrons separate in the metal due to contact with the electrolyte. Therefore, track insulation is essential for both interference current protection and preventing such corrosion.

In addition to traction currents, four key factors play a critical role in influencing the amount of stray current. The first factor is the conductance per unit length of the tracks and other parts of the return circuit. The second is the distance between substations. The third factor includes the longitudinal resistance of the running rails and the rail-to-earth conductance of a track section, which is influenced by factors like the type of fasteners, sleepers, and soil characteristics under different environmental conditions. Finally, the fourth factor is the spacing of cross bonds [5]. Another important element that affects stray current levels is the conductivity of both the surrounding soil and the track insulation.

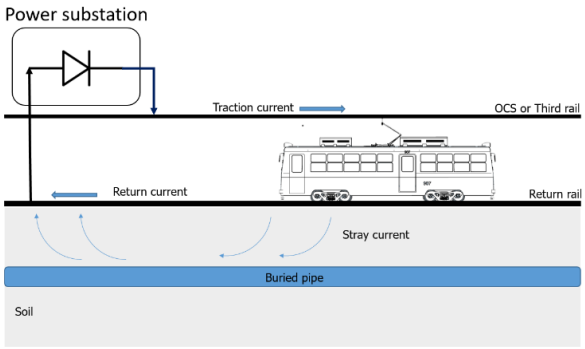

Figure 1. Stray current is generated in the traction system

To study the distribution characteristics of stray current, many researchers have developed various models for its estimation [6], [7]. For example, stray current can be estimated based on an impedance model [8]. Researchers categorize stray current simulations using different methods, including simplified theoretical models [9]. Several approaches exist for simulating stray current, such as the finite element method (FEM) (FEM) [10], [11], MATLAB-based simulations [12], [13], and current distribution, electromagnetic field, grounding, and soil structure analysis (CDEGS) simulations [14], [15]. In railway stations, partial differential equations derived from Maxwell's equations have been used to estimate stray current on platforms, applying FEM and simulation tools like COMSOL software [16], [17]. FEM is favored by many researchers due to its efficiency and flexibility in providing accurate solutions [18]-[20].

This research focuses on analyzing the distribution of stray current influenced by track insulation conductivity using the FEM approach, supported by computer-aided simulation tools, to provide a detailed understanding of how insulation conductivity affects current leakage into the ground. By varying the conductivity values of the track insulation, the study aims to identify critical thresholds where insulation performance significantly impacts stray current flow. The simulations consider different operational scenarios, including variations in fastener resistance and soil conductivity, to assess their combined effects on stray current distribution. Additionally, the study evaluates the role of soil depth and its influence on current dissipation, providing insights into how deeper soil layers reduce stray current concentration. The findings from this research will contribute to the development of more effective insulation strategies and rail system designs that minimize stray current leakage, thereby enhancing the safety and longevity of rail infrastructure.

2. METHOD

2.1. Track insulation measurement method

In line with track protection requirements [21], the key factor influencing stray currents departing from the tracks is the conductivity per unit length between the track and the ground. An important factor in risk assessment is the corrosion rate. Rail potential provides valuable insights into parameters related to stray currents, such as traction currents, the longitudinal resistance of the running rails, earth resistance, and the length of the feeding sections. A crucial requirement for this process is to ensure that no accidental or intentional direct electrical connection is made to grounding installations.

According to the EN50122-2 standard, the stray current per unit length should not exceed 2.5 mA/m (average stray current per length of a single-track line). If the conductance per unit length specified in EN50122-2, which is 0.5 S/km/track, is not exceeded, further investigations or specific measures are not required. The methods for measuring track conductance are outlined in the European standard EN50122-2. The track segment to be examined is isolated from continuous lines by insulated rail joints or rail nicks, and the section must not exceed 2 km in length. The conductivity per unit length of the isolated track section is determined using the method illustrated in Figure 2 and (1).

$$G_{RE} = \frac{1}{L} \times \frac{I}{U_{RE,on} - U_{RE,off}} \quad (1)$$

Researchers have simulated the rail-to-earth conductance per unit length of a single viaduct structure in accordance with the EN 50122-2 standard using MATLAB/Simulink [22]. The simulation aimed to calculate the rail-to-earth conductance per unit length based on the resistance values of the fasteners. The results of the simulation are shown in Table 1. The rail-to-earth conductance per unit length values

obtained in Table 1 will be used as parameters in simulating the stray current in the ground using the FEM. This simulation will help analyze the impact of varying rail-to-earth conductance per unit length.

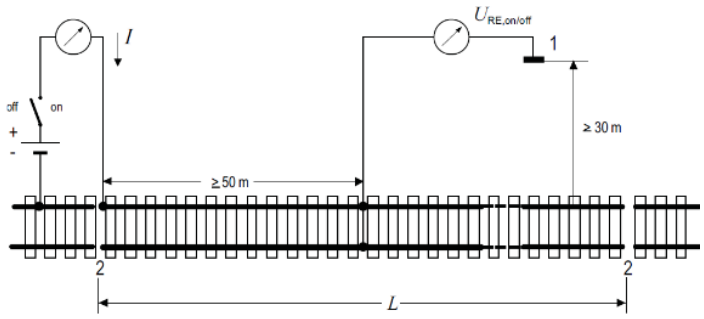

Figure 2. Conductance per length for track sections measurement using EN 50122-2 method

Table 1. The rail-to-earth conductance per unit length based on the resistance values of the fasteners [22]

No.	Fasteners (Ω)	G'$_{RE}$ (S/km)
1	100	13.341
2	300	7.275
3	500	5.001
4	700	3.81
5	900	3.077
6	1,000	2.807
7	2,000	1.495
8	3,000	1.019
9	4,000	0.773
10	5,000	0.623
11	6,000	0.521
12	7,000	0.448
13	8,000	0.393
14	9,000	0.35
15	10,000	0.316
16	100,000	0.032
17	1,000,000	0.0032
18	10,000,000	0.00032

2.2. Mathematical model for current conservation

The mathematical model represents the current conservation problem for the current source and can be applied to models. The current density is determined by fundamental equations, including Ohm's law, which governs current transfer density [23], [24].

$$\boldsymbol{J} = \sigma \boldsymbol{E} \tag{2}$$

$$\boldsymbol{E} = -\nabla V \tag{3}$$

$$-\nabla(\sigma \nabla V - J_e) = Q_j \tag{4}$$

Where J is current density (A/ m^2) σ is the electrical conductivity (S/m), E is the electric field (V/m), V is an electric potential (V), J_e is an externally generated current density (A/m^2), and Q_j is an external current source (A/m^3).

2.3. Solution using the finite element method

The FEM is a numerical technique used to obtain approximate solutions for a wide range of engineering problems. Among the numerous numerical methods developed over time, the finite difference method is one of the most widely used techniques, the finite volume method, and the FEM. In the FEM, the solution domain is divided into many small, interconnected sub-regions, or elements, providing a piecewise approximation to the governing equations. This means that the complex partial differential equations are reduced to either linear or nonlinear simultaneous equations. The discretization process in FEM, which

involves dividing the domain into smaller regions, converts a continuum problem with an infinite number of unknowns into a problem with a finite number of unknowns at specific points, known as nodes. Because the FEM allows for the flexible formation of these elements or sub-regions, it can closely represent the boundaries of complex domains.

2.4. Finite element method for stray current analysis

2.4.1. Define the geometry of the model

Figure 3 presents a simplified geometry of the DC tram traction system, with the parameters used in the simulation listed in Table 2. These parameters were carefully selected to ensure the accuracy and reliability of the solution, providing a realistic representation of the system's operational conditions.

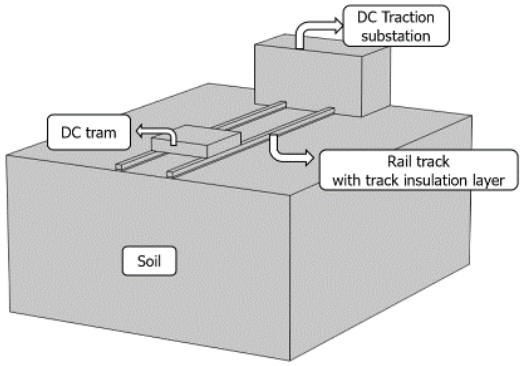

Figure 3. The geometric of the DC tram traction system

Table 2. Geometric parameter of the DC tram traction system

Geometric	Value (m)
Depth of soil	0.5
Length of soil	100
Position of train to station	60
Height of rail	0.2
Length of rail	100

The simulation domain for the FEM, utilizing linear tetrahedron elements, was generated using COMSOL software to create a structured mesh. The mesh comprises a total of 17,058 elements, as illustrated in Figure 4. This high-resolution mesh was carefully selected to ensure an accurate representation of the geometry while maintaining computational efficiency. The size and density of the mesh elements were refined in critical areas, especially around the boundaries where the potential for stray current concentration is higher. This refinement is crucial to accurately capture the complex electromagnetic behavior in the DC traction system. Mesh convergence analysis was performed to verify that the selected element count produces reliable results without excessively increasing the computational load. Furthermore, the boundaries were assigned appropriate conditions to simulate real-world interactions, such as conductivity values and insulation properties, providing a more comprehensive and realistic simulation environment.

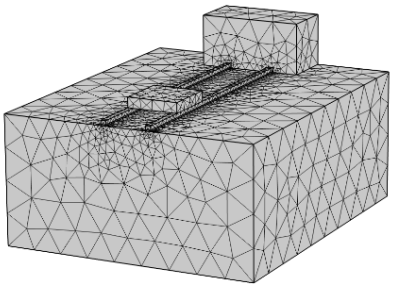

Figure 4. Generated mesh to DC tram traction system

2.4.2. Definition of the material property

For the model simulation using COMSOL software, material properties were specified for each component, including the DC tram, DC traction substation, rail track with fastening system, and surrounding soil. The key parameter for all components in this current conservation problem is the electrical conductivity (σ), which directly influences the stray current behavior and its distribution across the system. The values of electrical conductivity for each material are provided in Table 3, ensuring accurate representation of the electromagnetic properties within the simulation.

Table 3. Material properties [25]

Material	Conductivity(S/m)
rail track	5
DC tram	1
station	0.01
clayey wet soil	1×10^{-1}
Track insulation at Fastener resistance 1,000 Ω	2.8×10^{-3}
Track insulation at Fastener resistance 3,000 Ω	1.0×10^{-3}
Track insulation at Fastener resistance 6,000 Ω	0.5×10^{-3}

2.4.3. Boundary conditions

The boundary conditions must be carefully defined to ensure the accuracy of the simulation model. First, a zero electric potential is applied at the DC traction substation, serving as the reference point for current return. This establishes a baseline for the flow of electrical current throughout the system. Next, the current source data from a simple single-train simulation is applied as the boundary condition to represent the vehicle's peak current at the DC tram, as illustrated in Figure 5. To account for regions outside the modeled domain, electric insulation is applied at the outer boundaries to prevent current flow beyond the simulation area. Finally, the initial conditions are set by assigning a zero electric potential across the domain, allowing the simulation to start from a neutral state and accurately capture the dynamic behavior of the system.

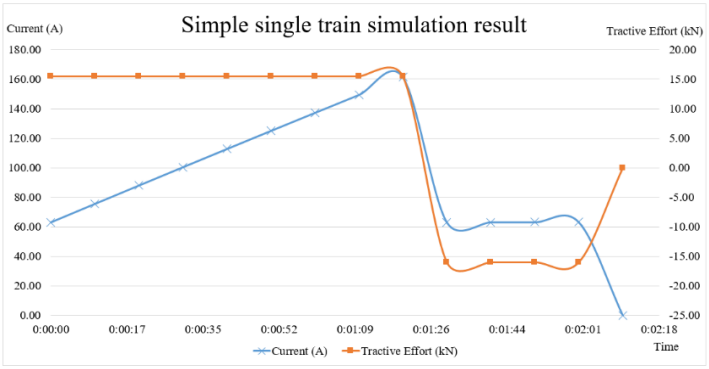

Figure 5. Current consumption results from a simple single train simulation

3. RESULTS AND DISCUSSION

The simulation results, derived from current conservation using the FEM in COMSOL software, display the current density across the model. These results clearly illustrate the distribution of stray current and electrical potential under various operational conditions, providing valuable insights into how current flows through different components of the DC tram traction system. The analysis highlights areas where stray current is concentrated, as well as regions with higher electrical potential, which are critical for assessing potential risks and optimizing system design for improved insulation and current return efficiency.

3.1. Stray current and rail potential under different track insulation

The simulation results were compared across three samples of track insulation conductivity, which depend on fastener resistance values of 1,000 Ω (2.8×10^{-3} S/m), 3,000 Ω (1.0×10^{-3} S/m), and 6,000 Ω (0.5×10^{-3} S/m), all based on a constant soil conductivity of 1×10^{-1} S/m. This comparison allows for an

assessment of how varying the fastener resistance affects the stray current distribution and overall system performance under identical soil conditions.

The simulation reference point for stray current density is compared across three samples of track insulation conductivity, each determined by the fastener resistance. The y-coordinate represents the specific location where the rail track makes contact with the soil, as illustrated in Figure 6. This comparison highlights how different fastener resistance values influence the distribution of stray current at the rail-soil interface, providing critical insight into the impact of track insulation on current leakage behavior.

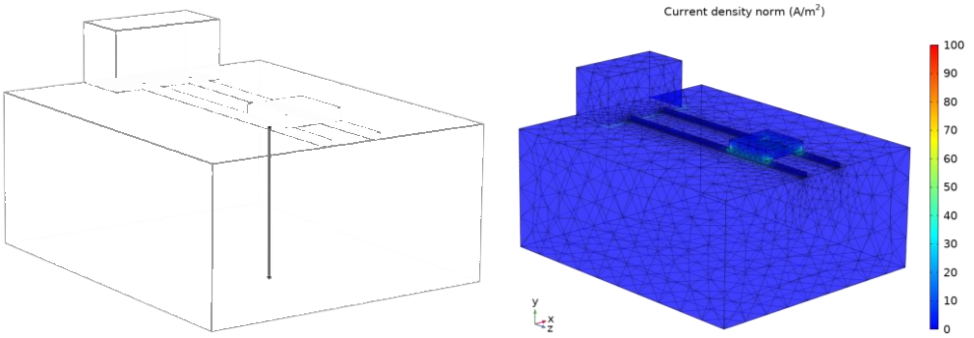

Figure 6. The reference position of the cutting plane along the y-coordinate is used to compare the results of stray current density

Figure 7 illustrates the current density results for track insulation conductivity based on a fastener resistance of 1,000 Ω (2.8×10^{-3} S/m). The simulation shows that the stray current density is highest at the y-coordinate, where the rail track contacts the soil, reaching a peak value of 5 A/m². This concentration of stray current at the rail-soil interface highlights the critical role of fastener resistance in managing current leakage.

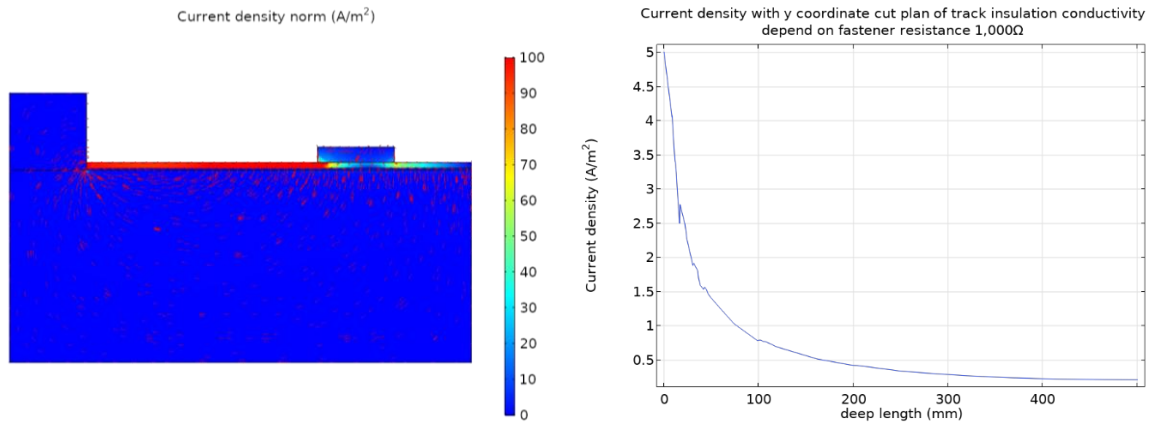

Figure 7. Distribution of stray current density in the 2-D cut plane system under track insulation conductivity, based on a fastener resistance of 1,000 Ω

Figure 8 presents the current density results for track insulation conductivity based on a fastener resistance of 3,000 Ω (1.0×10^{-3} S/m). The simulation indicates that the stray current density reaches its peak value of 4.5 A/m² at the y-coordinate, where the rail track contacts the soil. This reduction in stray current density compared to lower resistance values emphasizes the influence of increased fastener resistance on mitigating current leakage.

Figure 9 illustrates the current density results for track insulation conductivity based on a fastener resistance of 6,000 Ω (5.0×10^{-3} S/m). The simulation shows that the stray current density peaks at 1.8 A/m² at the y-coordinate, where the rail track contacts the soil. This significant reduction in stray current density, compared to lower resistance values, underscores the effectiveness of higher fastener resistance in minimizing current leakage at the rail-soil interface.

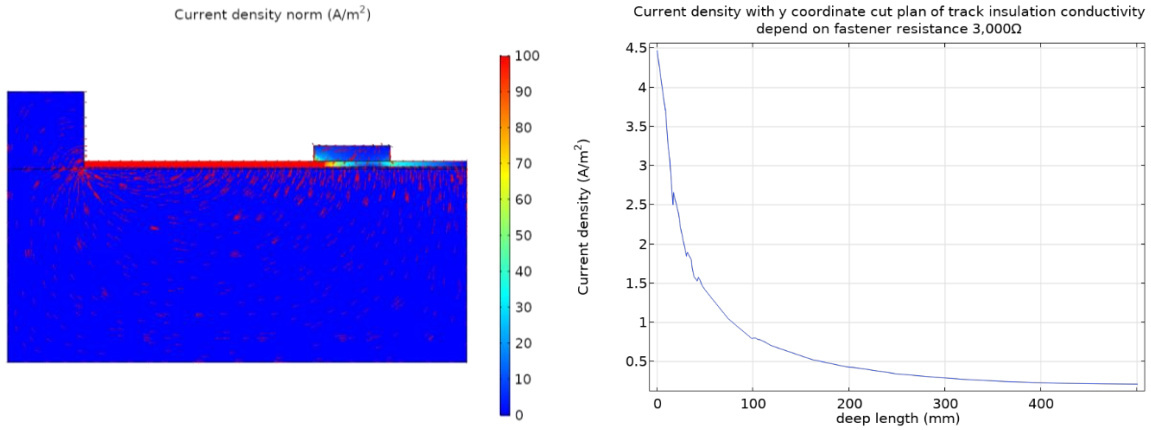

Figure 8. Distribution of stray current density and electric potential in the 2-D cut plane system, based on track insulation conductivity with a fastener resistance of 3,000 Ω

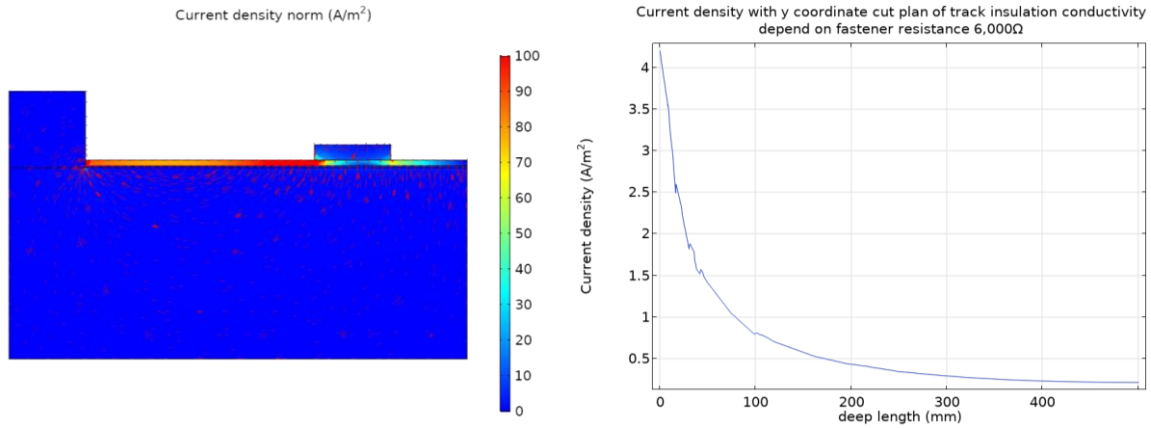

Figure 9. shows the distribution of stray current density and electric potential in the 2-D cut plane system, based on track insulation conductivity with a fastener resistance of 6,000 Ω

The stray current density results are analyzed along a cutting plane parallel to the y-coordinate, at a soil depth ranging from 0 to 0.5m, for three different cases of track insulation conductivity. The results demonstrate that variations in track insulation conductivity significantly influence stray current density. As the soil depth increases, the stray current density decreases, indicating that the depth of track insulation plays a crucial role in controlling current leakage into the surrounding soil.

4. CONCLUSION

In conclusion, this study successfully demonstrated the significant impact of track insulation conductivity on stray current density and electrical potential in DC tram traction systems. The FEM was employed to provide a detailed analysis of the interaction between the rail track and the surrounding environment. The results confirmed that lower track insulation conductivity leads to higher stray current densities, posing a potential risk to surrounding infrastructure and safety systems. Additionally, the study highlighted the importance of soil depth in mitigating stray current, as greater depths resulted in lower stray current densities.

These findings are valuable for optimizing track insulation and improving the design of rail systems to minimize stray current leakage, thus enhancing the longevity of the infrastructure and reducing safety risks. By accurately predicting the electrical potential of the return rail, this method offers a reliable tool for assessing touch voltage and informing protective measures against electrical hazards. Future research could expand on this work by investigating other factors influencing stray current, such as rail material properties, environmental conditions, and dynamic loading scenarios, to further refine protection strategies and improve system reliability.

ACKNOWLEDGMENTS

This work was supported by School of Electrical Engineering, Institute of Engineering, Suranaree, University of Technology.

FUNDING INFORMATION

Authors state no funding involved.

AUTHOR CONTRIBUTIONS STATEMENT

This journal uses the Contributor Roles Taxonomy (CRediT) to recognize individual author contributions, reduce authorship disputes, and facilitate collaboration.

Name of Author	C	M	So	Va	Fo	I	R	D	O	E	Vi	Su	P	Fu
Apiwat Aussawamaykin	✓	✓	✓	✓	✓	✓	✓	✓	✓	✓	✓			
Padej Pao-la-or	✓	✓		✓	✓	✓			✓	✓		✓	✓	✓

C : **C**onceptualization
M : **M**ethodology
So : **So**ftware
Va : **Va**lidation
Fo : **Fo**rmal analysis
I : **I**nvestigation
R : **R**esources
D : **D**ata Curation
O : Writing - **O**riginal Draft
E : Writing - Review & **E**diting
Vi : **Vi**sualization
Su : **Su**pervision
P : **P**roject administration
Fu : **Fu**nding acquisition

CONFLICT OF INTEREST STATEMENT

Authors state no conflict of interest.

DATA AVAILABILITY

The authors confirm that the data supporting the findings of this study are available within the article.

REFERENCES

[1] A. Aussawamaykin, A. Bunmat, and P. Pao-La-Or, "Finite element analysis of DC traction system stray current under different soil conductivity," in *Proceeding of the 2021 9th International Electrical Engineering Congress, iEECON 2021*, Mar. 2021, pp. 125–128, doi: 10.1109/iEECON51072.2021.9440328.

[2] G. Lucca, "Evaluating stray current interference from DC traction lines on a pipeline network by means of a stochastic approach," *Electrical Engineering*, vol. 103, no. 1, pp. 417–428, Aug. 2021, doi: 10.1007/s00202-020-01091-7.

[3] Y. Ni *et al.*, "Study on distribution characteristics of metro stray current," in *2021 IEEE International Conference on Electrical Engineering and Mechatronics Technology (ICEEMT)*, Jul. 2021, pp. 19–25, doi: 10.1109/ICEEMT52412.2021.9601438.

[4] M. Ormellese, S. Beretta, F. Brugnetti, and A. Brenna, "Effects of non-stationary stray current on carbon steel buried pipelines under cathodic protection," *Construction and Building Materials*, vol. 281, p. 122645, Apr. 2021, doi: 10.1016/j.conbuildmat.2021.122645.

[5] H. H. Quang, "EN 50122-2:2010: Railway applications - fixed installations - electrical safety, earthing and the return circuit - part 2: provisions against the effects of stray currents caused byDC traction systems." European Standard, 2010.

[6] G. Yang, X. Ma, and Z. Cao, "Modeling and dynamic analysis of uneven parameter metro stray current distribution," *Electrical Engineering*, vol. 106, no. 2, pp. 2021–2032, Oct. 2024, doi: 10.1007/s00202-023-02053-5.

[7] X. Yang, M. Wang, T. Q. Zheng, and X. Sun, "Modelling and simulation of stray current in urban rail transit—a review," *Urban Rail Transit*, vol. 10, no. 3, pp. 189–199, Sep. 2024, doi: 10.1007/s40864-024-00227-3.

[8] T. Chuchit and T. Kulworawanichphong, "Rail potential calculation between traction substations for dc railway systems (in Thai)," *Engineering Journal of Research and Development, The Engineering Institute of Thailand Under H.M. The King's Patronage (EIT)*, vol. 30, no. 3, pp. 57–71, 2019.

[9] C. Wang, W. Li, Y. Wang, S. Xu, and M. Fan, "Stray current distributing model in the subway system: a review and outlook," *International Journal of Electrochemical Science*, vol. 13, no. 2, pp. 1700–1727, Feb. 2018, doi: 10.20964/2018.02.16.

[10] M. Brenna, A. Dolara, S. Leva, and D. Zaninelli, "Effects of the DC stray currents on subway tunnel structures evaluated by FEM analysis," in *IEEE PES General Meeting, PES 2010*, Jul. 2010, pp. 1–7, doi: 10.1109/PES.2010.5589590.

[11] H. Zhong *et al.*, "The influence analysis of the power grid topology on the stray current invading transformers," in *2022 4th International Conference on Control and Robotics (ICCR)*, Dec. 2022, pp. 179–182, doi: 10.1109/ICCR55715.2022.10053889.

[12] Y. Wang, Z. Li, H. He, W. Lu, Y. Xu, and Y. Mao, "An inductance forcedly absorbing current circuit to reduce the stray current in the DC power supply system," in *2019 14th IEEE Conference on Industrial Electronics and Applications (ICIEA)*, Jun. 2019, pp. 2303–2308, doi: 10.1109/ICIEA.2019.8834227.

[13] P. Svoboda, S. Zajaczek, R. Sprlak, and J. Mohylova, "Simulation of stray currents on single track in Matlab Simulink," in *Proceedings of the 2014 15th International Scientific Conference on Electric Power Engineering (EPE)*, May 2014, pp. 609–612, doi: 10.1109/EPE.2014.6839484.

[14] N. Yan-Ru, Z. Xiang-Jun, Y. Kun, L. Yang, and P. Ping, "Research on modeling method of transformer DC bias caused by metro stray current," in *2018 International Conference on Power System Technology (POWERCON)*, Nov. 2018, pp. 3834–3839, doi: 10.1109/POWERCON.2018.8602113.
[15] Q. Li *et al.*, "Research on the influence of stray current on grounding grid and corresponding protection," in *2020 IEEE 4th Conference on Energy Internet and Energy System Integration (EI2)*, Oct. 2020, pp. 3631–3635, doi: 10.1109/EI250167.2020.9346612.
[16] S. Zajaczek, P. Svoboda, L. Ivanek, and R. Sprlak, "Examination of current fields in the vicinity of railway L - type platform," in *Proceedings of the 2014 15th International Scientific Conference on Electric Power Engineering (EPE)*, May 2014, pp. 625–629, doi: 10.1109/EPE.2014.6839434.
[17] S. Lin, Z. Tang, X. Chen, X. Liu, and Y. Liu, "Analysis of stray current leakage in subway traction power supply system based on field-circuit coupling," *Energies* , vol. 17, no. 13, p. 3121, Jun. 2024, doi: 10.3390/en17133121.
[18] P. Pao-La-Or and A. Bunmat, "Shielding of magnetic field effects on operators working a power transmission lines using 3-D FEM," *International Journal of Mechanical Engineering and Robotics Research*, vol. 8, no. 5, pp. 779–785, 2019, doi: 10.18178/ijmerr.8.5.779-785.
[19] S. Vacharakup, M. Peerasaksophol, T. Kulworawanichpong, and P. Pao-La-Or, "Study of natural frequencies and characteristics of piezoelectric transformers by using 3-D finite element method," *Applied Mechanics and Materials*, vol. 110–116, pp. 61–66, Oct. 2012, doi: 10.4028/www.scientific.net/AMM.110-116.61.
[20] C. Zhichao and H. Cheng, "Evaluation of metro stray current corrosion based on finite element model," *The Journal of Engineering*, vol. 2019, no. 16, pp. 2261–2265, Jan. 2019, doi: 10.1049/joe.2018.8653.
[21] "Railway applications - fixed installations - electrical safety, earthing and the return circuit - part 1: protective provisions against electric shock." European Standard, 2011.
[22] T. Chuchit and T. Kulworawanichpong, "Stray current assessment for DC transit systems based on modelling of earthing and bonding," *Electrical Engineering*, vol. 101, no. 1, pp. 81–90, Mar. 2019, doi: 10.1007/s00202-019-00758-0.
[23] S. Zajaczek, J. Ciganek, J. Mohylova, and M. Durica, "Modelling of stray currents near a railway platform," *Advances in Electrical and Electronic Engineering*, vol. 15, no. 5, pp. 763–769, Jan. 2018, doi: 10.15598/aeee.v15i5.2343.
[24] M. I. Mousa, Z. Abdul-Malek, and I. M. Zainab, "Leakage current based thermal modeling of glass disc insulator surface," *Indonesian Journal of Electrical Engineering and Computer Science (IJEECS)*, vol. 6, no. 3, pp. 504–512, Jun. 2017, doi: 10.11591/ijeecs.v6.i3.pp504-512.
[25] J. B. Rhebergen, H. A. Lensen, P. B. W. Schwering, G. R. Marin, and J. M. H. Hendrickx, "Soil moisture distribution around land mines and the effect on relative permittivity," in *Detection and Remediation Technologies for Mines and Minelike Targets VII*, Aug. 2002, vol. 4742, pp. 269–280, doi: 10.1117/12.479098.

BIOGRAPHIES OF AUTHORS

Apiwat Aussawamaykin is graduated student at the School of Electrical Engineering, Institute of Engineering, Suranaree University of Technology, Nahkon Ratchasima, Thailand. He received B.Eng. (2008) in electrical engineering from Rajamangala University of Technology Isan Khonkaen Campus, M.Eng. (2013) in electrical engineering, Rajamangala University of Technology Thanyaburi. His fields of research interest include a railway electrification system, finite element analysis, and renewable energy. He can be contacted at email: apiwat4321@gmail.com.

Padej Pao-la-or is an associate professor of the School of Electrical Engineering, Institute of Engineering, Suranaree University of Technology, Nakhon Ratchasima, Thailand. He received B.Eng. (1998), M.Eng. (2002) and D.Eng. (2006) in electrical engineering from Suranaree University of Technology, Thailand. His fields that interest is about the broad range of power systems, finite element analysis, optimization and artificial intelligence, electromagnetic field, electrical machinery and energy conversion. He has joined the school since December 2005 and is currently the member of Power System Research, Suranaree University of Technology. He can be contacted at email: padej@sut.ac.th.